Journal of Electric Propulsion

REVIEW Open Access

Reverberation chamber for electromagnetic compatibility testing of electric thrusters

F. Kiefer[1*], K. Holste[1], P. J. Klar[1], Y. Rover[2], U. Probst[2] and C. Volkmar[2]

Presented at the 37th International Electric Propulsion Conference Massachusetts Institute of Technology, Cambridge, MA USA June 19-23, 2022

*Correspondence: felix.kiefer@exp1.physik.uni-giessen.de

[1] Institute of Experimental Physics I, Justus Liebig University, Heinrich-Buff-Ring 16, Giessen 35392, Germany
[2] Center of Competence for Nanotechnology and Photonics (NanoP), TH Mittelhessen - University of Applied Sciences, Wiesenstrasse 14, Giessen 35390, Germany

Abstract

The need for electromagnetic compatibility (EMC) of electrical devices on satellites increases dramatically as the number of satellites is rapidly growing and the density of electrical devices on the satellite increases due to their miniaturization. Thus, EMC of the electric propulsion system becomes an important issue for a safe and reliable operation of the satellite. In particular, this also concerns the electric propulsion system. Since electric thrusters usually need to be operated in vacuum, dedicated facilities are required to assess their EMC. Here, we present how a common cylindrical vacuum vessel can be converted into a reverberation chamber suitable for EMC pre-compliance testing of electric thrusters. We describe and validate its operation principle and discuss its limitations. Finally, we show first measurement results of radiated emission measurements of a thruster and compare those with data obtained for the same thruster in a semi-anechoic chamber where the thruster is operated inside a metal-free vessel and fires into a larger vacuum chamber outside the semi-anechoic chamber.

Keywords: Electromagnetic interference testing, Electric propulsion, Electromagnetic compatibility, Reverberation chamber, Semi-anechoic chamber

Motivation and background

The demand for electric propulsion (EP) grows as space launches get more affordable and the number of satellite formations successfully commissioned increases rapidly. Commercialization drives this sector. On the one hand, time-to-market of space devices drastically needs to be reduced in order to be more cost effective. On the other hand, safe operation of devices, such as thrusters, on satellites in space must be ensured. Corresponding proofs of product quality and durability require exhaustive testing. In this context, interoperability becomes a major requirement as the density of electronic devices on satellites increases and the satellites themselves are further miniaturized [1]. EP systems like any other electronic devices also need to fulfill electromagnetic compatibility (EMC) requirements. The EMC properties of most electronics can be analyzed under ambient conditions. This is different in case of EP systems as electric thrusters need a space like vacuum environment for operation [2]. It is of particular interest to measure radiated emissions of an ion thruster in operation to assess its impact on the entire satellite system. The EP/EMC test laboratory operated by Justus Liebig University in cooperation with the University of Applied Sciences in Giessen (THM) comprises two

test facilities for assessing the EMC of electric thrusters and cube sat systems. Besides a semi-anechoic chamber (SAC) connected to a dedicated vacuum chamber, we have converted a cylindrical vacuum vessel into a reverberation chamber (RVC). Here, we describe the operation principle and design of our RVC test facility and present initial radiated emission measurements of a thruster.

Radiated EMC tests are typically performed in an anechoic chamber or a SAC. Furthermore, the relevant standards name RVCs as an alternative test facility, especially for electromagnetic susceptibility (EMS) testing [3]. In EMS investigations, the equipment under test (EUT) is exposed to electromagnetic (EM) radiation. To realize the specified EM field strength at the position of the EUT in a RVC, less power is needed compared to the same experiment inside a SAC. Thus, testing in a RVC facility becomes an interesting alternative, especially, if high field strengths are demanded [4]. However, when it comes to electromagnetic interference (EMI) tests, standards like MIL-STD [3] and ECSS [5], which apply for space applications, do not mention RVCs as suitable means for testing, but just SACs. Nevertheless, we will demonstrate that, in case of electric thrusters, a RVC facility has its merits when it comes to EMI measurements of EP systems. Furthermore, a metallic vacuum chamber used for standard testing of EP devices can be converted into a RVC with less effort and at a considerably lower price than setting up a SAC facility for EMC characterization of EP systems [2].

The operating principle of a RVC is based on a resonant cavity whose EM mode spectrum is perturbed by using stirring elements. The EM mode spectrum of a resonant cavity consists of discrete modes corresponding to standing waves or eigenmodes. The spatial dimensions of the cavity essentially determine these resonance frequencies or eigenfrequencies. To obtain a quasi-continuous frequency spectrum as a time-average, at least one stirring element is needed. It is typically a rotating metallic stirrer. Whilst rotating, it continuously changes the EM boundary conditions and thus alters the resonance frequencies [4]. Built-in broadband antennas convert EM fields into measurement signals, so that the entire RVC works as a nonlinear transducer for input power to internal field strength (EMS measurement). Alternatively, internal field strength can be converted to output power (EMI measurement). In both cases, the mode spectra measured and averaged for different stirrer positions yield a continuous mode spectrum, which, after an appropriate response correction, corresponds to an integral free-space spectrum. Thus, after proper calibration, the measured data can be converted into field strength measured at a specified distance in free space [6]. Since IEC61000 [7] designates a RVC an applicable facility for EMI measurements, the procedure described in this particular document can be applied for calibration. The main disadvantage of such a facility is the low cutoff frequency, which is given by its geometry. For a cylindrically shaped resonant cavity with a length l greater than its diameter d, the lowest frequency is determined by the TE_{111} mode [8, 9] and can therefore be approximated by

$$f_0 = \frac{1}{2\pi\sqrt{\mu_0\varepsilon_0}}\sqrt{\left(\frac{1.841}{d/2}\right)^2 + \left(\frac{\pi}{l}\right)^2} \tag{1}$$

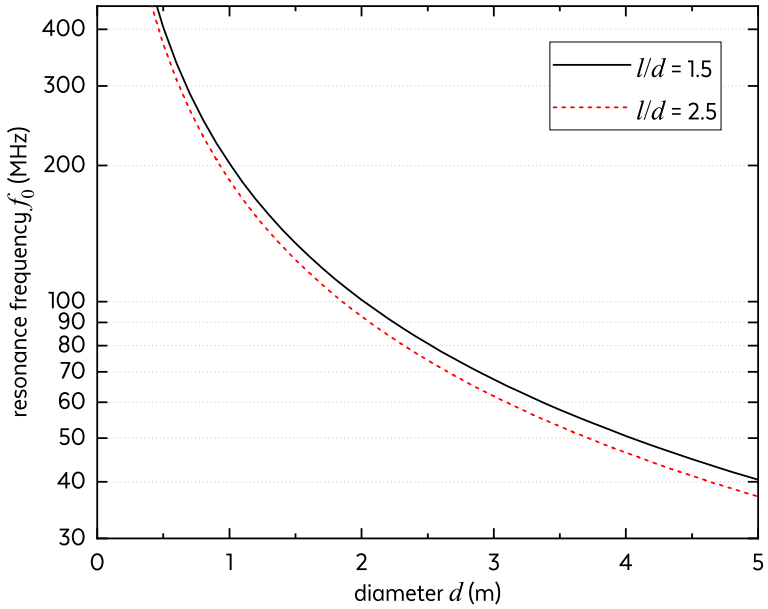

Fig. 1 Frequency f_0 of the TEM_{111} mode in a cylidrical RVC calculated as a function of chamber diameter d for different ratios of length to diameter l/d

For simplicity, we ignore that components like stirrers, antennas, the EUT itself and other built-in elements may affect this frequency. The lowest frequency $f_{\min}$ to perform EMI tests in a RVC is recommended to be at least three times its first resonant frequency, i.e., $f_{\min} > 3\, f_0$ [7]. Another definition for the low cutoff frequency demands at least 100 modes to evolve [3], which can be approximated using Weyl's equation [8]. It must be noted that Eq. (1) corresponds to a cylinder with flat caps and not torispherical heads, which are common for vacuum vessels. Hence, the length l in Eq. (1) must be considered an effective length. Ratios of $l/d = 1.5$ to 2.5 are typical for vacuum chambers of EP test facilities such as our vacuum vessels [10]. Figure 1 shows the dependence of f_0 on chamber diameter d assuming the given ratios of l/d.

Approach

A typical lower boundary of the transition frequency in EMI test procedures is 30 MHz [3, 5, 7]. This value should, in principle, be the aim for $f_{\min}$ when designing a new chamber. Figure 1 reveals that large chambers with a diameter of 5 m and a length of 7.5 m reach $f_0 \approx 40$ MHz allowing reliable RVC measurements to be performed above $f_{\min} > 120$ MHz. Even extending the chamber's length to 12.5 m does not reduce $f_{\min}$ below 100 MHz. Thus, a RVC with $f_{\min} \approx 30$ MHz is still challenging, but a $f_{\min}$ value of 100 MHz may be realized based on larger existing chambers. Thus, a restriction of the accessible frequency range (i.e., $f_{\min}$ defines the lower boundary) needs to be conceded when setting up a RVC for EMI measurements of thrusters.

To assess the feasibility of EMI testing in a RVC, we designed the cylindrical vacuum RVC shown in Fig. 2. The chamber has a diameter of 1.6 m and a length of about 2.4 m. The dedicated pumping system comprises of two backing pumps and one turbo-molecular pump and reaches an initial pressure lower than 10^{-6} mbar which rises to about 3×10^{-5} mbar at $Q = 0{,}25$ sccm Xe propellant flow into the chamber.

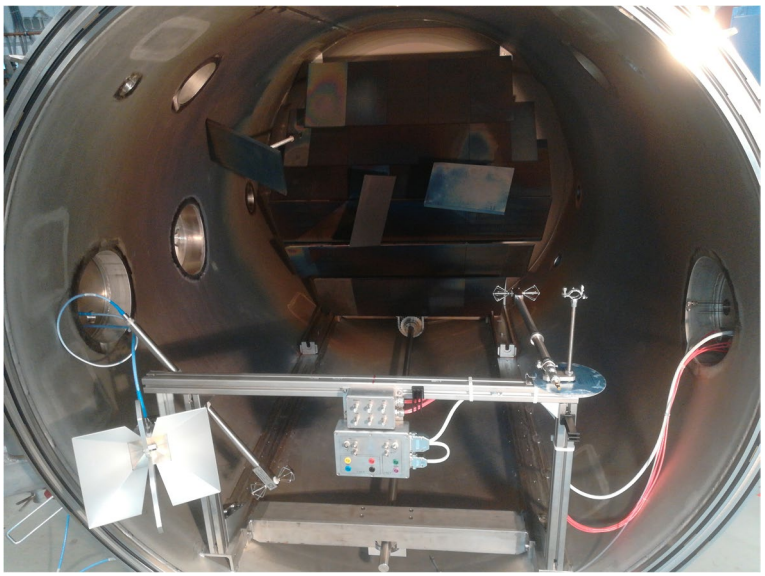

Fig. 2 View inside the vacuum RVC without EUT at Justus Liebig University Gießen

The laboratory is air-conditioned to minimize temperature influences on facility and feed system. According to Eq. (1), the lowest resonance is $f_0 \approx 126\,\text{MHz}$ for our vacuum chamber without installations, which corresponds to $f_{\text{min}} \approx 378\,\text{MHz}$. The vacuum chamber is equipped with a graphite beam dump, which is required for accommodating the power of the expelled ion plume of electric thrusters . To save space and cost, the RVC's field stirrers are part of the beam dump. Dedicated antennas rated for the range of 500 MHz to 18 GHz are available. However, these antennas allow measurements already starting from 300 MHz when conceding a lower gain. In our measurements, we focus on the range above 500 MHz, as the installations, in particular the beam dump, will increase f_0 and thus f_{min} slightly. Nevertheless, the RVC is calibrated over the entire frequency range from 300 MHz to 18 GHz. The calibration was performed according to IEC61000 [7] since MIL-STD [3] and ECSS [5] do not qualify RVCs for EMI measurements. The calibration procedure was managed by the commercial software EMC32 provided by Rohde & Schwarz just as the measurement procedure itself.

Figure 3 depicts a simplified simulation model of our RVC representing EMS measurement. Typically, the EUT will be an operating thruster and it will be mounted with its plume facing the beam dump with the stirrer unit. The stirrer unit consists of three mechanically coupled stirrer panels arranged such that the axial symmetry of the chamber is broken. Each stirrer panel is designed as a single plate with graphite protection. Despite its simplicity, this design ensures field turbulence as well as full-surface protection of each stirrer when in contact with the ion plume. The required antennas and the optional field probe are positioned next to or behind the EUT for protection.

The chamber response was simulated based on the computer-aided design (CAD) model shown, which allowed us to study the design of the stirrer unit before it was

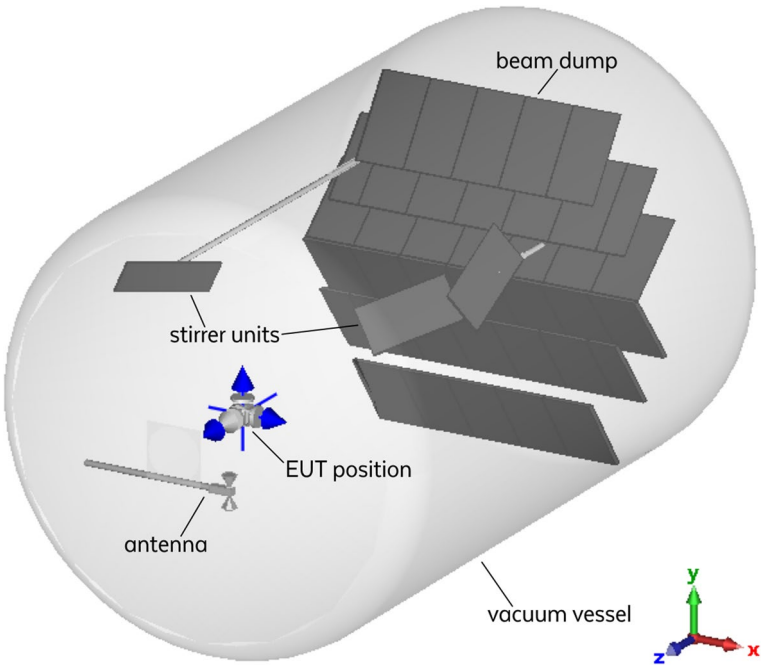

Fig. 3 Simplified EMS simulation model of our RVC with a stirrer angle defined as 18°

built and assembled. The simulation was carried out using Dassault Systèmes' Simulia software CST Studio Suite®. Broadband transient analyses were performed using the transmission-line matrix (TLM) method, which offers an octree-based meshing algorithm reducing the overall cell count [11] to about 100,000 in our model. Assuming all materials as perfect conductors and using a discrete face port, which replaces the antenna shown in Fig. 3, this software can efficiently solve single frequency problems for electrically large models using multilevel fast multipole method (MLFMM) calculations [11]. Results of the modelled EM behavior of the novel RVC chamber design and its stirrer unit are depicted in Fig. 4. As examples, two stirrer unit positions, referred to as positions 18° and 22°, were chosen to demonstrate the effect of the stirrers on the response of the RVC. The stirrer arrangement depicted in Fig. 3 corresponds to the 18° position.

Figure 4 shows the averaged amplitude in the central plane of the cylindrical test chamber for an excitation at a frequency of 475 MHz for the stirrer unit positions 18° and 22°.The average field strength at stirrer angle 18° is higher compared to that at stirrer angle 22°. The increase is caused by the fact that for the selected stirrer angle the mode spectrum of the RVC exhibits a resonance close to 475 MHz. Moving the stirrer position to 22° shifts this resonance to adjacent frequencies, so that 475 MHz is then off-resonance. A resonance situation for a given frequency leads to higher field strengths at positions where constructive interference occurs (antinodes) when using the same amplifier power in a RVC compared to a SAC. The mode spectrum for the standing EM waves inside a resonator is discrete. The movement of the stirrer unit changes the resonance condition, basically, by wobbling this mode spectrum in frequency. Since antinodes and nodes (where destructive interference occurs, i.e., the field strength is low) alternate in the spatial intensity pattern for a given frequency, the stirring moves the spatial

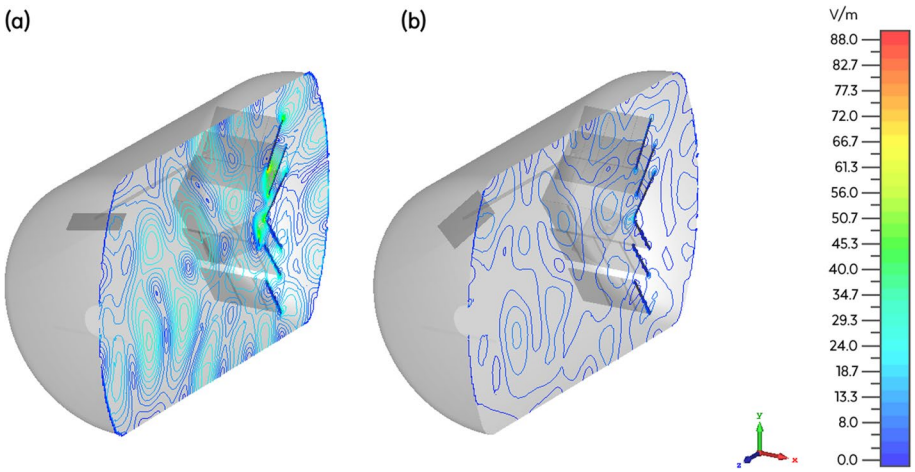

Fig. 4 E field plot of averaged absolute values for 475 MHz excitation on x_0-plane **a** for a stirrer angle of 18° and **b** of 22°

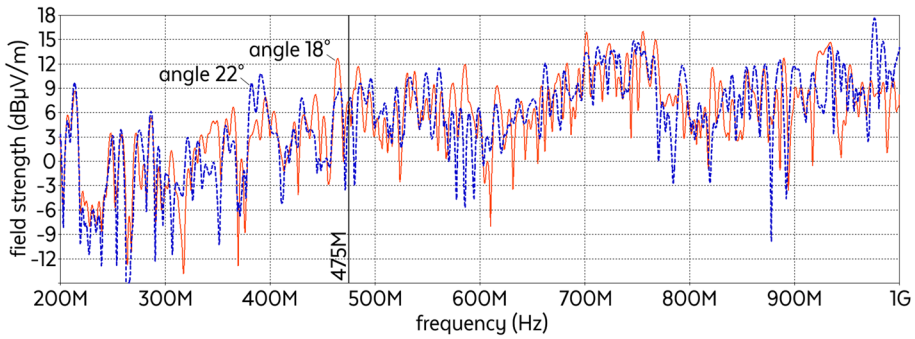

Fig. 5 Simulated spectrum of maximum absolute values of the E field at the location of the field probe in Fig. 3 for stirrer position 18° and 22° corrected for the antenna response

positions of nodes and antinodes during a measurement. This stirrer movement to the different discrete positions is supposed to ensure that antinodes of ideally all frequencies under study should occur in the spatial volume where the EUT is located. This has two purposes, first, to create a rather flat function of the time-averaged absolute EM field strength as a function of frequency at the position of the EUT and, second, to keep the average intensity level at the EUT position as high as possible during EMS measurement.

The influence of the stirrer unit becomes clearer when analyzing the behavior of the spectrum of maximum absolute field strength of the local E field at the location of the EUT. Figure 5 shows two such maximum amplitude spectra for the stirrer positions of 18° and 22°. The fact that moving the stirrer unit changes the electrical boundary conditions is reflected especially well by the behavior of the minima positions in the two plots. The frequencies corresponding to the minima, i.e., low field strength, vary between both stirrer positions. Most of the minima shift in frequency or vary in amplitude. Shifts in frequency imply that the resonance frequencies in the cavity resonator vary due to the stirrer motion. Changes in amplitude show that the intensities of the interfering waves yielding extinction at this frequency are somewhat different for the two stirrer positions, but not the actual condition for extinction itself. These

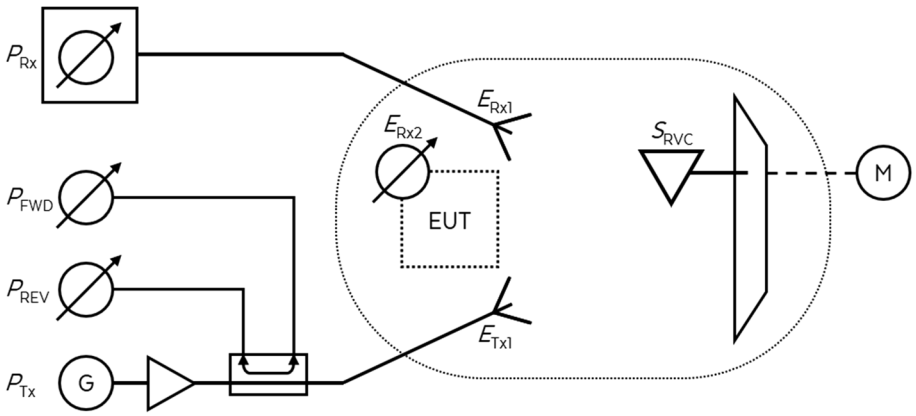

Fig. 6 Simplified schematic of the setup which was applied to calibrate the RVC according to IEC61000 utilizing EMC32 software from Rohde & Schwarz

two effects are coupled and cannot be considered independently of one another. The fact that minima can be shifted and their field amplitude changed by varying the stirrer position, indicates that the concept proposed for the stirrer unit here is viable.

The applied standard IEC61000 [7] specifies a minimum number of stirrer positions, which need to be incorporated in the chamber's calibration depending on the desired frequency range. One goal, when obtaining the chamber's response, is to validate whether the number of stirrer positions considered is sufficient for obtaining a smooth average spectrum, which is quasi continuous above $f_{\min}$. That way, it can be ensured that a significant field strength is realized at all frequencies in the desired operating range of the RVC.

The process of signal generation and detection in the calibration procedure is given in IEC61000 [7]. Figure 6 depicts the setup deployed for this purpose. At each sampling point in the frequency range of 300 MHz to 18 GHz, the following procedure is performed for 20 different discrete positions of the mode stirrer unit S_{RVC}. At each frequency f, a defined power P_{Tx} is coupled into the cavity resonator, i.e., the vacuum chamber. Amplitude of P_{Tx} is metered through P_{FWD} and P_{REV} with the help of a directional coupler. This power is transduced into an E field by a set of antennas E_{Tx1} (in the EMI measurements discussed in what follows, the EUT serves as the transducer, which couples its radiative power into the cavity resonator, instead of the antenna set E_{Tx1}). Internal reflections inside the cavity resonator lead to a standing wave field. A second set of built-in antennas E_{Rx1} connected to the spectrum analyzer receives the measurement signal P_{Rx} (which later will be dependent on the EMI of an EUT). In addition, an E field probe E_{Rx2} is installed, which measures the broadband field strength in the volume where the EUT will be placed. Following this procedure, a response $R_i(f)$ is recorded for each stirrer position i ($i = 1$ to 20). The system response $R(f)$ based on the collected calibration data is then computed as explained in IEC61000 [7] according to

$$R(f) = \max_{i=1 \text{ to } 20}\{R_i(f)\}. \tag{2}$$

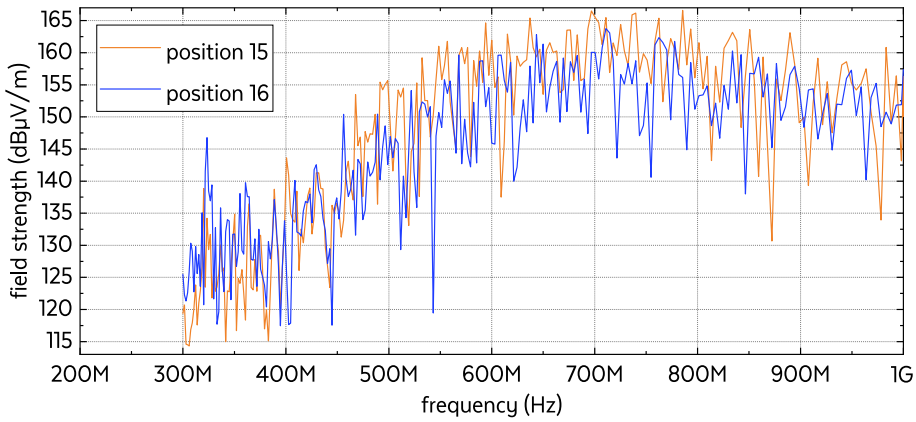

Fig. 7 Amplitude at receiving antenna E_{Rx1} during calibration, measured by spectrum analyzer ESW26 and transduced into field strength via antenna factor and cable losses for 2 W RF power input at each excitation frequency point

The same measurement procedure is then performed for the radiated emission of the EUT inside the chamber yielding the raw EMI spectrum (not corrected for the cavity resonator response)

$$S_{\mathrm{EUT,raw}}(f) = \max_{i=1 \text{ to } 20}\{S_i(f)\}. \tag{3}$$

The radiated emission spectrum S_{EUT} of the EUT is then obtained by normalizing to the system response

$$S_{\mathrm{EUT}}(f) = \frac{S_{\mathrm{EUT,raw}}(f)}{R(f)}. \tag{4}$$

In Fig. 7, we show two response spectra $R_{15}(f)$ and $R_{16}(f)$ corresponding to two stirrer positions, which are comparable with the positions used in the simulations leading to Figs. 4 and 5. Stirrer position 15 corresponds to simulation angle 18° and position 16 to angle 22°. The two measured response spectra exhibit the anticipated behavior. Maxima and minima occur as a function of frequency and the positions of the maxima and minima differ for the two stirrer positions in agreement with the simulations. The envelope of the simulated and the measured curves differs. However, this is anticipated as the simulations assume perfect materials and the underlying CAD model is simplified. Nevertheless, the comparison proves that the mode stirrer unit functions as desired.

Electrical tightness is another special requirement of a RVC besides its resonance frequency and field turbulence [2]. To shield EM fields from the surroundings, e.g., originating from radio stations, the measurement volume needs to be fully sealed and enclosed by highly conductive material. Copper gaskets, e.g. known from CF-flanges, are a suitable means to achieve both, vacuum and electrical tightness. For doors, which are opened frequently, e.g., to setup the EUT inside the chamber, rubber gaskets are more common since they do not need to be replaced after every opening of the chamber. The disadvantage is that rubber does usually not conduct electricity. Thus, a rubber seal provides a gap which allows EM waves from the outside to enter the vacuum chamber and possibly to interfere with measurement signals on the vacuum side. Such gaps

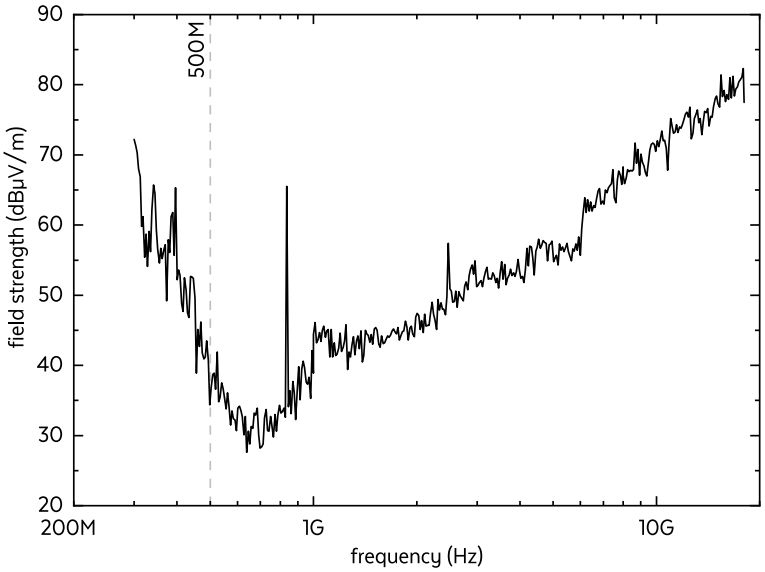

Fig. 8 Obtained RVC background noise at a virtual free space measurement distance of 1 m

can be closed by using special EMC gaskets, placed next to the rubber sealing. Figure 8 shows the measured noise floor inside the RVC translated into a virtual 1 m measurement distance in free space. The shape of this graph is characteristic for the frequency dependence of the sensitivity, since the transducer factor of the RVC (including cable losses, antenna factors and receiver parameters) is nonlinear and already corrected as mentioned above. Despite the electric sealing efforts, there are strong signals at two discrete frequencies visible in Fig. 8, one at about 840 MHz and the other at about 1.7 GHz, which correspond to leaks into our chamber. However, as the signals are very sharp, their impact on the analysis of the EM emission of the EUT is relatively small. Noting that the design focus was on using standardized flanges instead of best electrical shielding, this result is satisfactory.

Preliminary results

First measurements were performed with a PPT thruster as pre-compliance tests. This EUT was an engineering model of the PETRUS 1 J propulsion module designed by the Institute of Space Systems (IRS) at the University of Stuttgart for the CubeSat GreenCube. The propulsion module contains a cluster of four PETRUS pulsed plasma thrusters with a shared 1 J capacitor bank. As a fully integrated system, this EUT does not need a complex external feeding system apart from a voltage source and two communication wires.

Measurements in our RVC and SAC were performed with an EMI test receiver ESW26 from Rohde & Schwarz and controlled by appropriate software EMC32. As in the RVC, the initial pressure of our SAC is lower than 10^{-6} mbar, which rises to about 7×10^{-6} mbar at $Q = 0{,}25$ sccm Xe propellant flow. Since the PPT burns its onboard solid propellant, pulsed extractions, at here 2 Hz, have a rather negligible influence on the chamber's background pressure compared to systems with constant propellant inlet like a RIT. As mentioned above, the RVC was calibrated to be used in the range of 300 MHz to 18 GHz

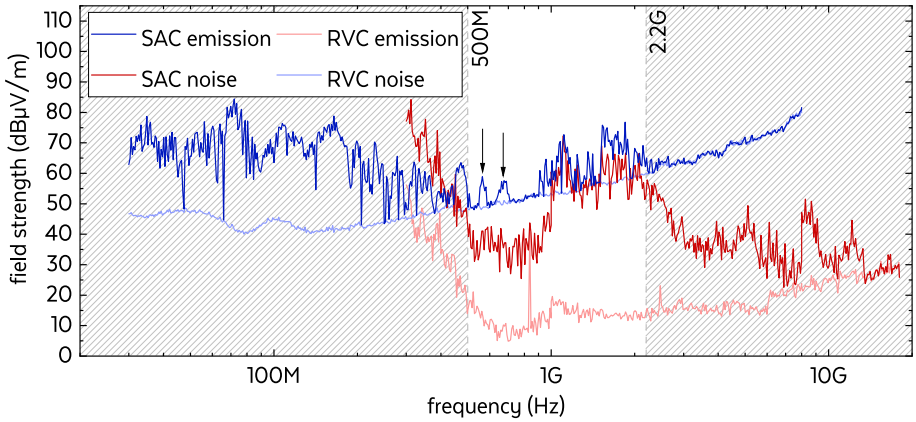

Fig. 9 Measured emissions of PPT Petrus 1 J (IRS) engineering model in SAC and RVC with related noise floors

based on IEC61000 [7] using 20 discrete stirrer positions. The measurement setup in the SAC is based on a logarithmic periodic broadband antenna covering 30 MHz to 8 GHz whose distance was 1.5 m from the EUT and was performed with the same instrument and software.

When considering the RVC as a calibrated transducer, the measurement result approximates the total radiated power of the EUT [8] integrated over all solid angles, converted into a measurable fraction at a virtual distance under free space conditions [6]. The RVC emissions were initially derived for 1 m virtual distance, which does not correspond to the utilized measurement distance of 1.5 m in the SAC. Therefore, the RVC emission data needed to be corrected for additional free space loss

$$\alpha(\Delta r) = \left(\frac{c_0}{4\pi f\ \Delta r}\right)^2 \tag{5}$$

over the distance $\Delta r = 0.5$ m [12]. Noise floors and data with the operating EUT measured with the RVC and SAC setups are depicted in Fig. 9. The EUT was operated under the same conditions in both facilities. The data of the RVC measurements are corrected for the additional free space loss as described above. Comparing both plots, the SAC's emissions are slightly above the RVC's, which already reflects the good correlation of the two data sets. The noise backgrounds of SAC and RVC facilities are different, in particular, due to differences of the procedures used for calculating the field strength. The lower noise floor of the RVC implies that this facility is more sensitive than the SAC setup in its current configuration. In particular, this seems to be the case at frequencies above about 2.2 GHz, where the measured field strengths of the operating EUT in the SAC measurement approaches and is comparable to the noise floor. In contrast, the field strengths of the EUT's EM emission can be reliably detected at frequencies above 2.2 GHz in the RVC measurement. It is not clear at the moment whether the sensitivity issue of the SAC setup can be improved significantly by using an preamplifier attached to the antenna or whether additional loss of sensitivity arises due to attenuation of EM waves with $f = 2.2$ GHz by the walls of the metal-free vessel surrounding the EUT. Currently, the EUT's emissions above 2.2 GHz seem to be below the noise floor of the SAC. Therefore, we cannot assure further assertions on data correlation above this frequency

by using those results. As pointed out above, the data of the RVC are only reliable above 500 MHz. Nevertheless, the data of both setups should be comparable in the intermediate range between 500 MHz and 2.2 GHz. It is worth noting that interference-like features are visible in this range in the SAC data: signals of the EUT rise above the noise floor at several narrow frequency bands (marked by the vertical arrows in Fig. 9) even though the RVC measurement does not indicate emissions with comparable magnitude. We will come back to this point in the discussion below.

The RVC response at the EUT at every frequency f above $f_{\min}$ arises from eigenmodes of the chamber for particular stirrer positions, if an antinode of the field occurs at the position of the EUT. As these eigenmodes are standing waves, the measured field strength corresponds to an integration over all solid angles yielding a spectrum of a virtual field strength derived for a specified distance to the EUT. On the one hand, the virtual field strength usually has a higher signal-to-noise ratio (SNR) with respect to the noise floor than in a SAC setup, which is advantageous. However, if the EUT's emission towards the receiving antenna inside the SAC has a high gain, the measured field strength may still in some cases exceed that measured inside the RVC. On the other hand, angle-resolved information is lost in the RVC, which is, in principle, accessible in a SAC measurement as the field strength measured inside a SAC represents the emission of the EUT into a solid angle segment along a specified spatial direction towards the antenna by varying the antenna position on a hemisphere about the EUT. In conventional EMI measurements in SACs, the EUT shall be rotated stepwise around all spatial axes in order to capture the worst case EMI of the EUT. This is not possible in case of the SAC systems used for studying electric thrusters. The reason is that there are not enough degrees of freedom for rotating the thruster inside the vacuum chamber needed for thruster operation. This reflects that the measurement principles in RVC and SAC setups are intrinsically different.

In what follows we will more carefully compare the measurement data of both setups in the intermediate frequency range between 500 MHz and 2.2 GHz. Since we are dealing with field strengths, the subtraction of the corresponding background noise from the two sets of emission data of operating EUT can be performed according to

$$\Delta E_{dB} = \left|E_{1,dB} - E_{2,dB}\right| = 20\log\left|10^{E_{1,dB}/20} - 10^{E_{2,dB}/20}\right|. \tag{6}$$

The background-corrected data obtained are plotted in Fig. 10. We have highlighted data values with a signal-to-noise ratio $SNR > 110\%$, defined as

$$SNR = \frac{E_{emission}}{E_{noise}}, \tag{7}$$

in the plot. Both sets of corrected data agree very well in in this intermediate frequency range given by the limitations of both setups, i.e., lower frequency boundary of 500 MHz in case of the RVC and a higher frequency boundary of 2.2 GHz in case of the SAC. The variation between the two curves is rather small, when considering that both measurement approaches operate on different principles. As already pointed out above, these are an integral measurement of the total emitted energy of the EUT [8] inside the RVC, which is translated into a field strength at a specific measurement distance in free space,

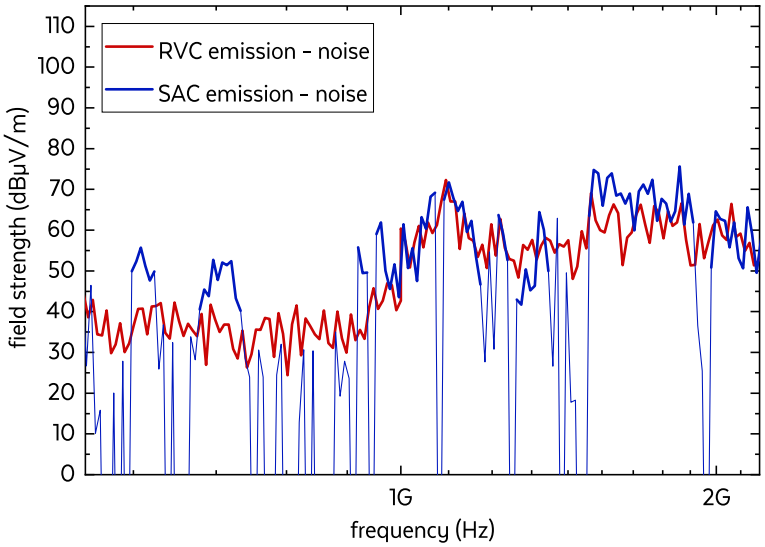

Fig. 10 Extraction of emission results with $SNR > 110\%$ (bold lines) and $SNR \leq 110\%$ (narrow lines) of PPT Petrus 1 J (IRS) engineering model in SAC and RVC with subtracted noise floors

and a direct measurement at this distance under free space-like conditions inside a SAC. A possible explanation of the interference-like features in the SAC data is the following. Since the SAC has no absorbers mounted on the floor, ground reflections may occur. This corresponds to an additional path for the radiated emission, which may interfere constructively or destructively at the position of the receiving antenna with the radiated emission travelling directly along the free space path towards the antenna. The phase shift between the two paths depends on frequency (wavelength) leading to the interference oscillations in measured spectra [12]. An alternative explanation may be that the metal-free vessel surrounding the EUT inside the SAC plays a role in this context, as its walls need to be passed by the radiated emission of the EUT. Our long-term goal is further improving measurement procedures including correction methods in order to allow us to extract the free-space radiated emission of the EUT from measurements under laboratory conditions.

Conclusion

A vacuum chamber transformed into a RVC offers suitable means of assessing the radiated emissions of an EUT that requires vacuum conditions for operation. The EUT may be an electric thruster or even a small cubesat system with an EP system. The dimensions of the vacuum chamber converted into the RVC define the lower boundary f_{min} of the accessible frequency range of the EMI measurement inside the RVC. Essentially, it holds, the larger the chamber, the lower is the cutoff frequency f_{min}. Due to its operating principle, a RVC is more sensitive regarding low emission power compared to approaches using (semi-) anechoic chambers. Despite the different noise margin, both facilities studied here, the RVC setup and SAC setup used as reference, deliver comparable results of the same thruster used as EUT running at the same defined operating point in both setups. The measurement procedures for assessing the EMI properties of electric thrusters defined in the relevant standards are based on SAC facilities. However,

our preliminary results suggest that EMI measurements of electric thrusters in RVCs can yield similar results than SAC-based approaches. Thus, RVC measurements turn out to be a useful approach for pre-compliance testing of EMI and a viable alternative to SAC experiments. Despite these promising first results, further experiments are needed to clarify whether EMI measurements of electric thrusters in RVCs are fully equivalent to SAC approaches and may be treated on an equal level in future standards referring to EP testing and qualification.

Nomenclature

f_0	lowest resonance frequency of a cavity resonator
$f_{\min}$	lowest working frequency to comply EMC requirements
d	diameter of a cylindrical cavity
l	length of a cylindrical cavity
$\alpha(\Delta r)$	free space attenuation pending on distance difference
SNR	signal-to-noise ratio adapted on electric field results

Acknowledgements
This project is supported by funds of "Bundesministerium für Wirtschaft und Energie" (BMWi) under grant no 50RS1903 and „Bundesministerium für Bildung und Forschung" (BMBF) under grant no 13FH173PX8. Furthermore, EU regional funding via the EFRE scheme of the State of Hesse is gratefully acknowledged. Special thanks go to F. Schaefer from the Institute of Space Systems (IRS) at the University of Stuttgart for providing the EUT and authorizing the publication of the measurement data.

Code availability
Simulations were performed using Dassault Systèmes' (3DS) Simulia software CST Studio Suite on release version 2021.02. Measurements were performed using Rohde & Schwarz' software EMC32 on version 11.40.00.

Authors' contributions
F. Kiefer gathered simulation and measurement results and drafted the manuscript. P. J. Klar provided facilities and equipment through EFRE as well as BMWi funds 50RS1903, supervised the project and contributed to the final version of the manuscript. K. Holste and Y. Rover supported the project organization. So did U. Probst and C. Volkmar and provided additional measurement equipment through BMBF funds 13FH173PX8. The authors read and approved the final manuscript.

Funding
Open Access funding enabled and organized by Projekt DEAL. This project is supported by funds of "Bundesministerium für Bildung und Forschung" (BMBF) under grant no 13FH173PX8, "Bundesministerium für Wirtschaft und Energie" (BMWi) under grant no 50RS1903 and EU regional funding via the EFRE scheme of the State of Hesse.

Availability of data and materials
https://doi.org/10.22029/jlupub-4187

Declarations

Competing interests
The authors declare that they have no known competing financial interests or personal relationships that could have influenced the work reported in this paper.

Received: 5 August 2022 Accepted: 23 January 2023
Published online: 02 March 2023

References

1. Holste K et al (2020) Ion thrusters for electric propulsion: Scientific issues developing a niche technology into a game changer. Rev Sci Instrum 91:061101. https://doi.org/10.1063/5.0010134

2. Zhang H et al (2020) Spacecraft Electromagnetic Compatibility Technologies – Space Science and Technologies Series. Beijing Institute of Technology Press and Springer Nature Singapore Pte Ltd., pp 65–66 473–474
3. Interface Standard (2015) MIL-STD-461G: Requirements for the control of electromagnetic interference characteristics of subsystems and equipment. Department of Defense, USA
4. Gustrau F, Kellerbauer H (2015) Elektromagnetische Verträglichkeit, Berechnung der elektromagnetischen Kopplung, Prüf- und Messtechnik, Zulassungsprozesse. Carl Hanser Verlag, Munich, pp 235–236
5. European Cooperation for Space Standardization (2012) ECSS-E-ST-20-07C Rev. 1: Space engineering – Electromagnetic compatibility. ECSS Secretariat ESA-ESTEC, Noordwijk
6. Boyes SJ, Huang Y (2016) Reverberation Chambers – Theory and Applications to EMC and Antenna Measurements. John Wiley & Sons Ltd., Chichester, pp 114–117
7. International Standard (2011) IEC61000-4-21: Electromagnetic compatibility (EMC) – Part 4-21: Testing and measurement techniques – Reverberation chamber test methods. International Electrotechnical Commission
8. Hill DA (2009) Electromagnetic Fields in Cavities – Deterministic and Statistical Theories. IEEE Press published by John Wiley & Sons, Inc., Hoboken, pp 25–47 122–127
9. Zinke O, Brunswig H (2000) Hochfrequenztechnik 1 – Hochfrequenzfilter, Leitungen, Antennen, 6th edn. Springer-Verlag GmbH, Berlin Heidelberg, pp 354–356
10. Justus-Liebig-University Website (2022) Testanlagen Übersicht – Testanlagen an der JLU Gießen. URL: https://www.uni-giessen.de/fbz/fb07/fachgebiete/physik/institute/ipi/raumfahrtphysik/Ionentriebwerke/testanlagen (retrieved June 1, 2022)
11. 3DS SIMULIA Software Package (2021) CST Studio Suite® Help – Electromagnetic Field Simulation Software, Release Version 2021.02, Dassault Systèmes
12. Detlefsen J, Siart U (2012) Grundlagen der Hochfrequenztechnik, 4th edn. Oldenbourg Wissenschaftsverlag GmbH, Munich, pp 229-233

Publisher's Note